

# CELLULAR STRUCTURES DETERMINED BY POLYGONS AND TREES

SATYAN L. DEVADOSS AND RONALD C. READ

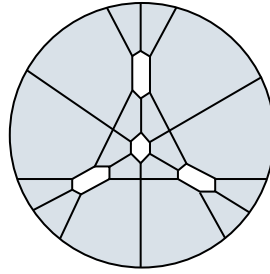
ABSTRACT. The polytope structure of the associahedron is decomposed into two categories, types and classes. The classification of types is related to integer partitions, whereas the classes present a new combinatorial problem. We solve this, generalizing the work of [25], and incorporate the results into properties of the moduli space  $\overline{\mathcal{M}}_0^n(\mathbb{R})$  studied in [8]. Connections are discussed with relation to classic combinatorial problems as well as to other sciences.

## 1. THE REAL MODULI SPACE

**1.1.** The Riemann moduli space  $\mathcal{M}_g^n$  of surfaces of genus  $g$  with  $n$  marked points has become a central object in mathematical physics. Introduced in Algebraic Geometry, there is a natural compactification  $\overline{\mathcal{M}}_g^n$  of these spaces; their importance was emphasized by Grothendieck in his famous *Esquisse d'un programme* [12]. The special case when  $g = 0$ , the space  $\overline{\mathcal{M}}_0^n(\mathbb{C})$  of  $n$  punctures on the sphere  $\mathbb{C}\mathbb{P}^1$ , is a building block leading to higher genera. They play a crucial role in the theory of Gromov-Witten invariants and symplectic geometry. Furthermore, they appear in the work of Kontsevich on quantum cohomology, and are closely related to the operads of homotopy theory. We look at the *real* points  $\overline{\mathcal{M}}_0^n(\mathbb{R})$  of this space; these are the set of fixed points under complex conjugation. This moduli space will provide the motivation to study certain combinatorial objects.

**Definition 1.1.1.** The real *Deligne-Knudsen-Mumford* moduli space  $\overline{\mathcal{M}}_0^n(\mathbb{R})$  is a compactification of the configurations of  $n$  labeled points on  $\mathbb{R}\mathbb{P}^1$  quotiented by the action of  $\mathbb{P}\mathrm{GL}_2(\mathbb{R})$ .

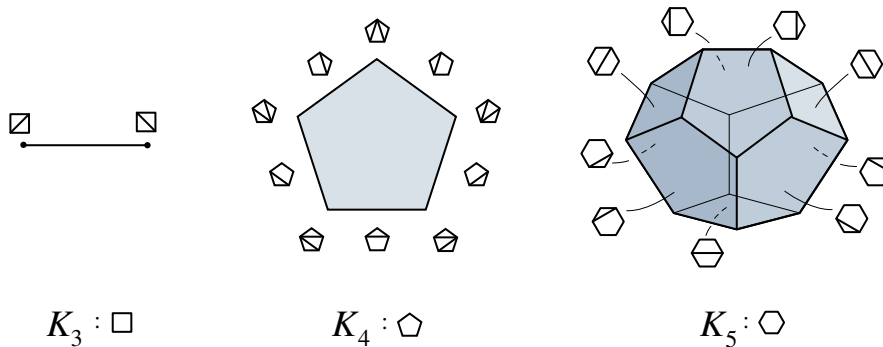
$\overline{\mathcal{M}}_0^n(\mathbb{R})$  is a manifold without boundary of real dimension  $n - 3$ . The moduli space is a point when  $n = 3$  and  $\mathbb{R}\mathbb{P}^1$  when  $n = 4$ . For  $n > 4$ , these spaces become non-orientable. Figure 1 shows  $\overline{\mathcal{M}}_0^5(\mathbb{R})$  (shaded) as the connected sum of five copies of  $\mathbb{R}\mathbb{P}^2$ , with the four hexagonal ‘boundaries’ and the outer circle carrying antipodal action. In general,  $\overline{\mathcal{M}}_0^n(\mathbb{R})$  can be described as the iterated blow-ups of real projective spaces (see [16, §4], [8, §4]), getting extremely complicated as  $n$  increases.

FIGURE 1.  $\overline{\mathcal{M}}_0^3(\mathbb{R})$ 

*Remark.* The diagram shown in Figure 1 is first found in the work of Brahana and Coble in 1926 [5, §1], relating to possibilities of maps with twelve five-sided countries.

**1.2.** A beautiful fact about the moduli space is its tiling by the convex polytope known as the associahedron  $K_n$ . It is the geometric realization of the poset of all meaningful bracketings on  $n$  variables. Originally defined for use in homotopy theory by Stasheff [30, §2], it was later given a convex polytope realization by Lee [17]. We use an alternative definition:

**Definition 1.2.1.** The *associahedron*  $K_n$  is a convex polytope of dim  $n - 2$  with codimension  $k$  faces corresponding to using  $k$  non-intersecting diagonals on an  $(n + 1)$ -gon.

FIGURE 2. Associahedra  $K_3$ ,  $K_4$  and  $K_5$ 

**Example 1.2.2.** The associahedron  $K_2$  is a point. Figure 2 shows the associahedra  $K_3$ ,  $K_4$ , and  $K_5$ . For instance, the polytope  $K_4$  is a pentagon whose sides (codim one faces) are labeled with 5-gons with one diagonal and whose vertices (codim two faces) are labeled with 5-gons with two diagonals.<sup>1</sup>



FIGURE 3. Polygons and clusters

We redraw our pictures of dissected polygons so that every region of the dissection becomes a regular polygon *without* diagonals. In the nomenclature of [25], we denote the resulting object as a *cluster*, where each regular polygon of the cluster is called a *cell*. Thus the polygon shown in Figure 3a with five diagonals is redrawn as a cluster in Figure 3b having six cells. Clearly dissected polygons and clusters are equinumerous, and it is sometimes easier to work with clusters rather than with dissections, as the following important property of the associahedron demonstrates.

**Proposition 1.2.3.** [30, §2] *Each face of  $K_n$  is a product of lower dimensional associahedra.*

**Example 1.2.4.** We look at the top (codim one) faces of  $K_5$ . The three-dimensional  $K_5$  corresponds to a 6-gon, which has two distinct ways of adding a diagonal. One way, in Figure 4a, shows the 6-gon as a cluster of two 4-gon cells; each cell corresponds to the line segment  $K_3$ , where the product of two such is a square. Alternatively, Figure 4b illustrates the other type of face, which is the product of  $K_2$  (point) and  $K_4$  (pentagon).

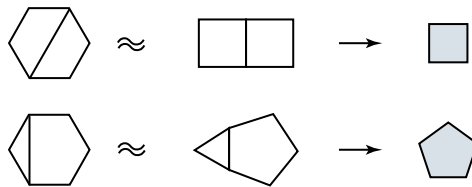


FIGURE 4. Codim one faces of  $K_5$

**1.3.** It was shown in [8, §2] that  $\overline{\mathcal{M}}_0^n(\mathbb{R})$  is tessellated by exactly  $\frac{1}{2}(n-1)!$  copies of  $K_{n-1}$ . For example, observe from Figure 1 that  $\overline{\mathcal{M}}_0^5(\mathbb{R})$  is tiled by twelve  $K_4$  pentagons. The reasoning is as follows: There are  $n!$  possible ways of labeling the sides of an  $n$ -gon, each corresponding to an associahedron. However, since there exists a copy of the dihedral group  $D_n$  of order  $2n$  in  $\mathbb{P}G\ell_2(\mathbb{R})$ , and since  $\overline{\mathcal{M}}_0^n(\mathbb{R})$  is defined as a quotient by  $\mathbb{P}G\ell_2(\mathbb{R})$ , two labeled polygons (associahedra) are identified

<sup>1</sup>Mention of *diagonals* will henceforth mean non-intersecting ones.

by an action of  $D_n$ . Therefore, in some sense, each associahedral domain of  $\overline{\mathcal{M}}_0^n(\mathbb{R})$  corresponds to a labeled  $n$ -gon up to rotation and reflection.

**Definition 1.3.1.** Let  $\mathcal{G}(n, k)$  be the set of equivalence classes of *labeled* regular  $n$ -gons with  $k$  diagonals up to the action of  $D_n$ . Let  $G$  be an element of  $\mathcal{G}(n, k)$  and  $d$  be a diagonal of  $G$ . The *twist* of  $G$  along  $d$ , denoted by  $\nabla_d(G)$ , is the polygon in  $\mathcal{G}(n, k)$  obtained by separating  $G$  along  $d$  into two parts, ‘twisting’ (reflecting) one of the pieces, and gluing them back (Figure 5). It does not matter which piece is twisted since the two results are identified by an action of  $D_n$ .

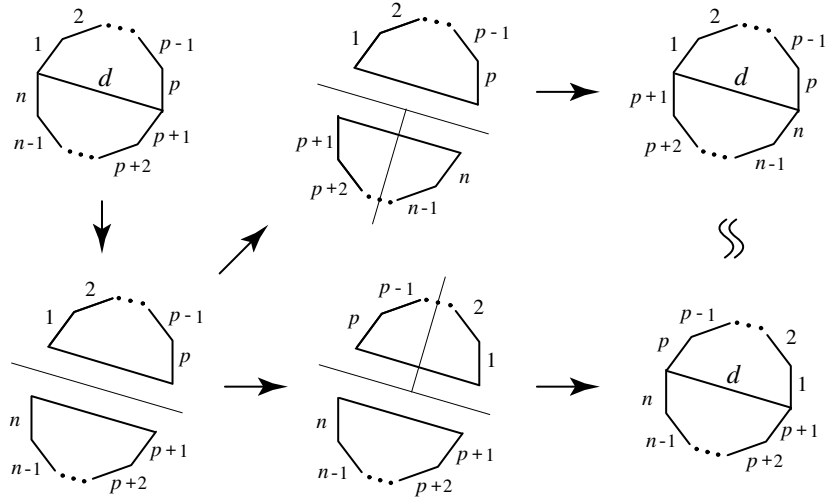


FIGURE 5. *Twist along  $d$*

**Theorem 1.3.2.** [8, §4] *Two labeled polygons,  $G_1, G_2 \in \mathcal{G}(n, k)$ , representing codim  $k$  faces of associahedra, are identified in  $\overline{\mathcal{M}}_0^n(\mathbb{R})$  if there exist diagonals  $d_1, \dots, d_r$  of  $G_1$  such that*

$$(\nabla_{d_1} \cdots \nabla_{d_r})(G_1) = G_2.$$

The previous statement shows how copies of associahedra glue together to form the moduli space. Figure 6 demonstrates  $\overline{\mathcal{M}}_0^4(\mathbb{R})$  tiled by three  $K_3$  line segments.

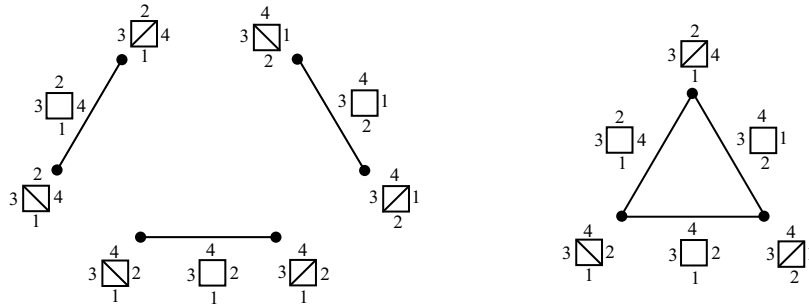


FIGURE 6. Copies of  $K_3$  and  $\overline{\mathcal{M}}_0^4(\mathbb{R})$

2. CATEGORIES OF FACES

2.1. Recall that faces of associahedra can be represented by dissected polygons. We give the following definitions that categorize the faces of  $K_n$ .

**Definition 2.1.1.** Two polygons  $G_1$  and  $G_2$  are of the same ...

*dimension* if their corresponding faces are of the same dimension.

*type* if their corresponding faces are the same polytope.

*class* if they are identified under the actions of  $D_n$  and twisting.

Dimension, type and class are in increasing order of finer partitions.

**Example 2.1.2.** In Figure 7, we note the difference between the categories of polygons belonging to  $K_5$ . Recall that the number of diagonals of a polygon is equal to the codim of its face; polygons (a) and (b) are of dim two, and (c) through (e) are of dim zero. In particular, polygons (c) through (e) are of the same type (points) whereas (a) and (b) are not; the polytope (a) is a square and (b) a pentagon. Only (d) and (e) are of the same class; that is, twisting along a diagonal of (d) will result in (e).

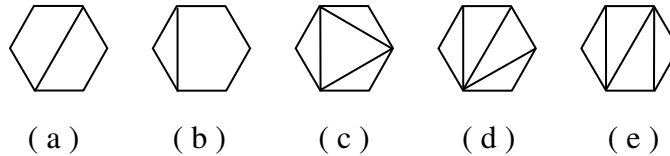


FIGURE 7. Different faces of  $K_5$

It makes sense to decompose the faces into dimensions and polytopes, but what does it mean to talk about classes? The two different classes of points discussed above correspond to the following: At one class (c), three pentagons meet; there are two such points in  $K_5$ . The other class (d) is where two pentagons and one square meet; there are twelve such points. Therefore, classes categorize *the different*

ways polytopes intersect in  $K_n$ . This idea can be extended to better understand the structure of  $\overline{\mathcal{M}}_0^n(\mathbb{R})$ .

**2.2.** The combinatorics involving dimensions are handled in [8]. We recall

**Lemma 2.2.1.** *The number of faces in  $K_n$  of codim  $k$  is*

$$\frac{1}{k+1} \binom{n+k}{k} \binom{n-2}{k}.$$

*In other words, given the  $f$ -vector of the polytope  $K_n$  to be  $f = (f_0, \dots, f_{n-3})$ , the number above is  $f_{n-k-2}$ .*

*Proof.* This was originally proved by Professor A. Cayley in 1891 in finding the number of partitions of an  $(n+1)$ -gon into  $k$  parts [6]. The recent work of Przytycki and Sikora gives a short and elementary proof while providing relations to knot theory [23].  $\square$

*Remark.* The number of faces in  $K_n$  of codim  $n-2$  is the well-known Catalan number  $c_n = \frac{1}{n+1} \binom{2n}{n}$ . That is, there are  $c_n$  vertices in the associahedron  $K_n$ . It is interesting to note that Stanley shows sixty-six ways to represent the Catalan numbers [29, Exercise 6.19].  $\square$

These are the three fundamental problems addressed in this paper:

- P1.* How many different types/classes of codim  $k$  are there in  $K_n$  ?
- P2.* What are the different types/classes in  $K_n$  of codim  $k$ ?
- P3.* How many faces of  $K_n$  belong to a given type/class?

In some sense, faces of the associahedron correspond to polygons and faces of the moduli space to *labeled* polygons. Therefore, since types and classes were defined regardless of labeling, the answers to *P1* and *P2* both carry over to the moduli space. This is not the case for *P3*. However, we find in [8] a formula (that follows from Theorem 1.3.2) which addresses this dilemma.

**Proposition 2.2.2.** *Let  $\Lambda(k, \mathfrak{X})$  denote the number of codim  $k$  faces in the CW-complex  $\mathfrak{X}$ . Then*

$$\Lambda(k, \overline{\mathcal{M}}_0^{n+1}(\mathbb{R})) = \frac{n!}{2^{k+1}} \cdot \Lambda(k, K_n).$$

**2.3.** In what follows, we find solutions to our fundamental problems regarding the classification of types. We try to clarify the situation with the following example.

**Example 2.3.1.** Looking at the case of  $K_6$ , Lemma 2.2.1 shows there to be 14 codim one faces. Figure 8 shows there to be two different types of such faces (answers *P1*), one being  $K_6$  and the other a pentagonal prism (answers *P2*). Out of the 14 faces, there turn out to be seven faces of each type (answers *P3*).

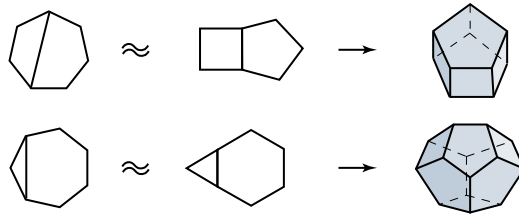


FIGURE 8. Codim one faces of  $K_6$

Polygons are of the same type if their corresponding associahedral faces have identical polytopal structure. As Proposition 1.2.3 indicates, the polytope structure is solely determined by the number of different cells, not the way these cells are glued to form the cluster. The following notation is well-defined: A face is of type  $\langle 3^{m_3} : 4^{m_4} : \dots \rangle$  if it corresponds to a cluster that has  $m_i$  number of  $i$ -sided cells. The superscript  $m_i = 1$  as well as the terms with  $m_i = 0$  are omitted. For example, the three types in Figure 7 are, respectively,

$$\langle 3^0 : 4^2 \rangle = \langle 4^2 \rangle \quad \langle 3^1 : 4^0 : 5^1 \rangle = \langle 3 : 5 \rangle \quad \langle 3^4 \rangle.$$

Define  $p_k(n)$  to be the number of partitions of  $n \in \mathbb{N}$  into exactly  $k$  integers  $n_1, \dots, n_k$ , where  $n_i > 0$  and  $n = n_1 + \dots + n_k$ . There is no closed form for  $p_k(n)$  but the following recurrence relation provides a means to calculate it:

$$(2.1) \quad p_k(n) = p_{k-1}(n-1) + p_k(n-k).$$

**Theorem 2.3.2** (Solution to *P1* and *P2*). *The number of different types in  $K_n$  of codim  $k$  is  $p_{k+1}(n-1)$ . The different partitions correspond to the different types, where  $n-1 = n_1 + \dots + n_{k+1}$  is associated with the polytope  $K_{n_1} \times \dots \times K_{n_{k+1}}$ .*

*Proof.* An  $(n+1)$ -gon with  $k$  diagonals (that is, a cluster containing  $k+1$  cells) represents a codim  $k$  face of  $K_n$ . The type of a face depends on the polytope structure; this is solely determined by the cells forming the cluster, *not* the way in which they are arranged to form the  $(n+1)$ -gon. Associating an  $(n+1)$ -gon to the integer  $n-1$ , observe that partitioning the polygon into  $k+1$  cells is identical to partitioning the integer into  $k+1$  parts.  $\square$

**Theorem 2.3.3** (Solution to *P3*). *When  $k = -1 + \sum m_i$  and  $n = 1 + \sum (i-2)m_i$ , the number of faces in  $K_n$  of type  $\langle 3^{m_3} : 4^{m_4} : \dots \rangle$  is*

$$\frac{1}{k+1} \binom{n+k}{k} \frac{(m_3 + m_4 + \dots)!}{m_3! m_4! \dots}.$$

*Proof.* This is proven by Goulden and Jackson [13, Exercise 2.7.14]. Their argument is similar to the proof given below for the enumeration of  $A$ -clusters (see §3.1), but without the twist operation and with the extra variables  $m_i$  in the generating function to mark the numbers of  $i$ -sided regions. From the recursive equation for the

generating function, the coefficients (functions of  $m_i$ ) are obtained by Lagrange's theorem and then expanded using the multinomial theorem.  $\square$

Values computed are shown in Table 1 using Equation 2.1. For each size of polygon, and each distribution of sizes of the cells in the dissection, it gives the number of polygons which have that distribution. An example of an entry for the partition of a 10-gon shows that there are 660 polygons of type  $\langle 3^2 : 4 : 6 \rangle$ . That is, there are 660 faces in  $K_9$  that have the polyhedral structure of  $K_2 \times K_2 \times K_3 \times K_5$ .

### 3. CLASSES AND THE COMBINATORICS OF TWISTING

**3.1.** Unlike types, the problem with regard to classes is no longer classical. Counting the number of dissected polygons up to rotation and reflection was studied in [25].<sup>2</sup> The difference now comes from imposing the additional equivalence relation of twisting. The method used to enumerate classes naturally follows as an extension of [25].

**Definition 3.1.1.** A cluster is said to be *rooted at an outside edge* if one edge (the *root*) of its perimeter is distinguished from the others. Figure 9a shows the root edge as a thicker line. For convenience, we refer to clusters rooted at an outside edge as *A-clusters*.

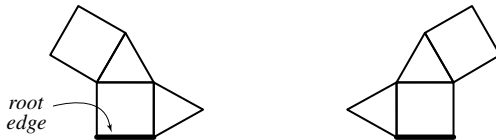


FIGURE 9. Outside root edge

Let  $a_{m,n}$  be the number of *A*-clusters having  $m$  cells and  $n$  outside edges not counting the root edge. Define the generating function

$$(3.1) \quad A(x, y) = \sum a_{m,n} x^m y^n,$$

where for the moment the limits for  $m$  and  $n$  are unspecified. For an *A*-cluster, there will be one cell with the root edge on its boundary; we can call this the *root cell*. Assume this cell has  $k$  unrooted edges. At each of these edges we have the option of gluing the root of some *A*-cluster to it.<sup>3</sup> Each of these glued clusters contributes its values of  $m$  and  $n$  to those of the resulting *A*-cluster. For the edges of the root cell at which nothing was glued, the contributions to  $m$  and  $n$  are 0 and 1 respectively. Hence the generating function  $A(x, y)$  will contain the term  $y$ . In the rest of  $A(x, y)$ ,  $m$  goes from 1 upwards and  $n$  from 2 upwards.

<sup>2</sup>This is equinumerous to the set of *outerplanar graphs*.

<sup>3</sup>This gluing is identical to the composition map for operads in the context of rooted trees.

We now have a typical Pólya-class problem.<sup>4</sup> There are  $k$  sites around the root cell at each of which we can place a figure, an  $A$ -cluster or just an edge, and the parameters  $m$  and  $n$  are additive. The figure counting series is the function  $A(x, y)$  just defined. To accommodate the twisting operation, we must regard an  $A$ -cluster as being equivalent to the one obtained by reversing the root edge — as in Figure 9a and 9b. This reversal interchanges the sites in pairs if  $k$  is even; if  $k$  is odd then one site remains fixed while the others interchange in pairs. Hence the cycle-index for this problem is

$$\begin{aligned} \frac{1}{2}(s_1^{2\alpha} + s_2^\alpha) & & k = 2\alpha \\ \frac{1}{2}s_1(s_1^{2\alpha} + s_2^\alpha) & & k = 2\alpha + 1. \end{aligned}$$

By Pólya's theorem, the generating function for  $A$ -clusters for which the root cell has  $k$  unrooted edges is obtained by putting  $s_1 = A(x, y)$  and  $s_2 = A(x^2, y^2)$  in the appropriate formula above. Summing for  $k$  from 2 upwards we get a function of  $s_1$  and  $s_2$ ,

$$\frac{1}{2} \sum_{k \geq 2} s_1^k + \frac{1}{2}(1 + s_1) \sum_{\alpha \geq 1} s_2^\alpha,$$

which reduces to

$$\frac{1}{2} \left[ \frac{s_1^2}{1 - s_1} + \frac{(1 + s_1)s_2}{1 - s_2} \right].$$

By substituting  $s_1 = A(x, y)$  and  $s_2 = A(x^2, y^2)$  in this expression, multiplying by  $x$  to account for the root cell, and adding the term  $y$  which we know must be present, we recover the generating function  $A(x, y)$  for  $A$ -clusters. This gives the recursive equation

$$(3.2) \quad A(x, y) = y + \frac{1}{2} \left[ \frac{A(x, y)^2}{1 - A(x, y)} + \frac{(1 + A(x, y))A(x^2, y^2)}{1 - A(x^2, y^2)} \right].$$

The occurrence of  $A(x^2, y^2)$  in this equation makes it impossible to obtain a closed form for the coefficients  $a_{m,n}$  but they can be successively computed as far as one wishes (see Table 2).

*Remark.* Another proof of Lemma 2.2.1 is obtained by computing the corresponding result above when twisting is *not* allowed. Then the relevant permutation group is the identity group, with cycle-index  $s_1^k$ , and the analog of Equation 3.2 is

$$V(x, y) = \sum v_{m,n} x^m y^n = y + \frac{xV^2(x, y)}{1 - V(x, y)},$$

where the numbers  $v_{m,n}$  are the counterparts to the  $a_{m,n}$  under the new conditions. In this case, as was shown in [25], a closed result is possible:

$$v_{m,n} = \frac{1}{m} \binom{n-2}{m-1} \binom{m+n-1}{n}.$$

---

<sup>4</sup>For information on such problems, see [21], [22], [27].

That is,  $v_{m,n}$  is the number of codim  $m - 1$  faces in  $K_n$ ; values are given in Table 3.

**3.2.** We now turn to clusters rooted at a cell, denoted as  $B$ -clusters. Figure 10 shows a typical  $B$ -cluster, having a distinguished cell (shown shaded) called the *root cell*. A  $B$ -cluster is obtained by gluing  $A$ -clusters (including possibly the empty  $A$ -cluster) by their roots to the edges of the root cell. If the root cell is  $k$ -sided, we have a Pólya-class problem for which the figure counting series is  $A(x, y)$  and the permutation group is the dihedral group  $D_k$ .

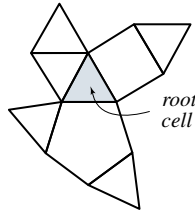


FIGURE 10. Root cell

Since the twisting operation is allowed, the way that the  $A$ -clusters are attached is not important. For this reason we are spared the tiresome necessity of distinguishing between symmetric and asymmetric clusters which had greatly complicated the enumerations performed in [25]. The cycle-index of  $D_k$  is

$$\begin{aligned} \frac{1}{2k} \sum_{r|k} \varphi(r) s_r^{k/r} + \frac{1}{4} (s_1^2 s_2^{\alpha-1} + s_2^\alpha) & \quad k = 2\alpha \\ \frac{1}{2k} \sum_{r|k} \varphi(r) s_r^{k/r} + \frac{1}{2} s_1 s_2^\alpha & \quad k = 2\alpha + 1. \end{aligned}$$

The  $B$ -clusters for a given value of  $k$  are enumerated by substituting  $A(x, y)$  in this cycle-index to get the generating function denoted by  $Z(D_k, A(x, y))$ . Hence the set of all  $B$ -clusters is enumerated by

$$B(x, y) = \sum_{m,n} b_{m,n} x^m y^n = x \sum_{k \geq 3} Z(D_k, A(x, y)).$$

There seems to be no way of simplifying this expression, but the coefficients can be easily computed as far as desired. Some values for  $b_{m,n}$  are given in Table 4.

**3.3.** The next enumeration is for clusters rooted at an inside edge which are asymmetrical about that edge; that is, for which the two clusters at the edge are different (Figure 11). Clearly these  $C$ -clusters, as they can be called, are formed by gluing together two different  $A$ -clusters, neither of which is the empty cluster, at their root edges.

Pólya's theorem shows the generating function for these clusters would be obtained by substituting  $A(x, y) - y$  in the cycle-index of the symmetric group  $\mathbb{S}_2$ ,

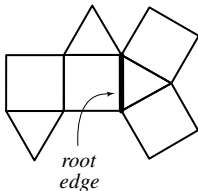


FIGURE 11. Inside root edge

namely  $\frac{1}{2}(s_1^2 + s_2)$ , but for the fact that we want the two  $A$ -clusters to be different. A variant of Pólya's theorem, which is well-known but in any case easily verified, provides the required result by substituting instead in the expression  $\frac{1}{2}(s_1^2 - s_2)$ . Calling the resulting generating function  $C(x, y)$ , we have

$$C(x, y) = \frac{1}{2}[(A(x, y) - y)^2 - (A(x^2, y^2) - y^2)].$$

The final step, going from the generating function for cell-rooted clusters to *free* clusters (those not rooted at all), is carried out by means of a theorem originally due to Otter [19] (also see [14], [25, §4]). It states that the generating function for these free clusters, call it  $F(x, y)$ , is obtained by subtracting  $C(x, y)$  from  $B(x, y)$ . The number  $f_{m,n}$  of clusters with  $m$  cells and  $n$  outside edges, is found from

$$F(x, y) = B(x, y) - C(x, y) = \sum f_{m,n} x^m y^n.$$

Some values for  $f_{m,n}$  are given in Table 5. We have just proved

**Theorem 3.3.1** (Solution to *P1*). *The number of different classes of  $K_n$  of codim  $k$  is  $f_{k+1, n+1}$ .*

#### 4. TREES AND THE COMPLEX MODULI SPACE

**4.1.** As a help in the study of the various classes, we prepared a set of drawings of the corresponding dissected polygons up to ten vertices. Figures 22 - 26 illustrate the different classes, labeled as  $n.k.i$  to denote an  $n$ -gon with  $k$  diagonals where  $i$  ranges from one to  $f_{n+1, k+1}$ . The computer algorithm for doing this was nothing out of the ordinary, but a few comments on how the drawings were produced may be of some interest. We exploited the connection between dissected polygons and trees as illustrated in Figure 12.<sup>5</sup> Trees dual to dissected polygons are *homeomorphically irreducible*, having no vertices of degree two.<sup>6</sup> Henceforth, mention of trees will imply homeomorphically irreducible ones. To each dissected polygon, we associate a tree imbedded in the plane. For each diagonal of the polygon, there is a tree edge connecting the two vertices on either side. The twist operation corresponds to reflecting one of the two subtrees at the ends of a given edge. Classes correspond

<sup>5</sup>Considering dissected polygons as plane graphs, we obtain trees by taking their *weak dual*.

<sup>6</sup>They are also known as *topological* or *reduced* trees.

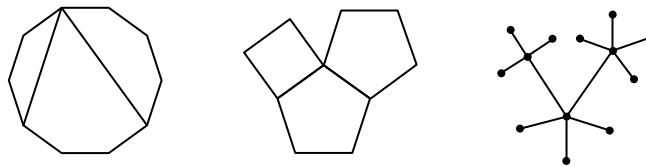


FIGURE 12. Polygons, clusters, and trees

to planar imbeddings of trees up to twisting. In other words, for a given class, each vertex of the tree is given the additional information of preserving the cyclic order of edges around that vertex. The problem was therefore to produce one such tree for each class.

Since the trees needed were quite small, it was not worth devising a clever algorithm; both elegance and efficiency were sacrificed for ease of programming. Rooted trees, the root being a vertex of the tree, were generated step by step according to height. There is one tree of height zero, and those of height one are the stars<sup>7</sup> with three or more edges at the root. Those of height two were obtained by grafting a subtree of height at most one, by its root, to the terminal vertices of these stars. In general, trees of height  $k$  were obtained by grafting trees of height at most  $k - 1$ . At each stage, if two trees were reflections of each other, only one was retained, thus taking care of the twist operation. This corresponds to producing clusters rooted at an edge, which made possible a check that the right numbers of trees were being produced.

The resulting lists of rooted trees would usually contain several copies of the same unrooted tree. The unwanted duplicates were weeded out by computing for each tree a *code* similar to that described in [26] and eliminating all but one of those with the same code. The actual program contained some refinements to the procedure just described but we shall skip the details. It was a fairly simple task to go from trees to dissected polygons. The diagrams<sup>8</sup> were then produced automatically using programs that had already been developed for the production of the book *An Atlas of Graphs* [28].

**Proposition 4.1.1** (Solution to *P2*). *The different classes correspond to the different pictures in Figures 22 - 26.*

At a later stage we decided to compute for each class the number of fixed dissections of that class. Had we thought of this earlier, it could have been done more easily along with the generation of the classes, but as it was, we derived these numbers directly from the data on the dissected polygons. For each such polygon,

<sup>7</sup>Also known as a *corolla*, a star is a collection of edges meeting at a common vertex.

<sup>8</sup>Although diagrams were created for ten-sided polygons, we do not include them here for the sake of space.

we produced the fixed polygons obtainable from it by rotations or by combinations of the twist operation. Note that twisting about some chords leaves the diagram unchanged, in which case there is no point in performing the twist. For example, those chords which have a single polygon on one side fall into this category, and are easily recognised. For ease of programming, only the chords of this kind were exempted from the twist operation; no attempt was made to recognize any others. As a result, duplicates could, and were, produced. However, for polygons with at most ten sides there can be at most five such chords, so the number of duplicates was small. They were eliminated by a suitable coding procedure, similar to that mentioned above for trees. It is reassuring that by summing these numbers for the appropriate sets of classes we recover the numbers given in Table 1.

**Proposition 4.1.2** (Solution to *P3*). *The number of faces of  $K_n$  of a particular class is indicated in the top right-hand corner of each picture in Figures 22 - 26.*

**4.2.** As mentioned above, there is a duality between clusters and trees. Clearly each cell of a cluster corresponds to a star in the tree. A face of the associahedron of a given type only recognizes the set of stars, not the way in which they are grafted to form the tree. However, a given class not only sees the underlying tree, but the additional cyclic order of edges around each vertex. Hence, faces of associahedra can be categorized by types, trees, and classes, in increasing order of refinement.

**Example 4.2.1.** Figure 13 shows three different trees and their corresponding (dual) polygons. All of them are of the same type  $\langle 4^2 : 5 \rangle$  and all fall into different classes. Note, however, that the first two correspond to the same tree, whereas the third does not. By not preserving the cyclic order of edges, we obtain a distinction that falls between the categories of type and class.

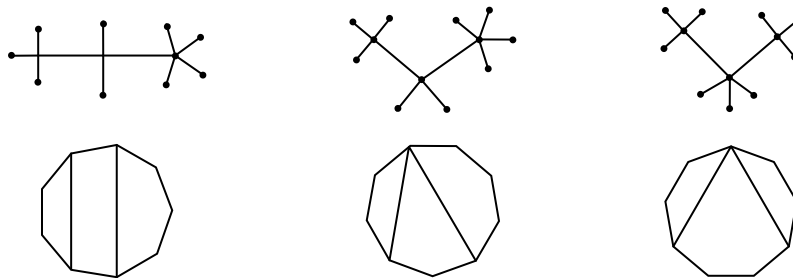


FIGURE 13. Some faces of  $K_8$  and their trees

The enumeration of all trees (not just homeomorphically irreducible ones) by their degree partitions is given by Harary and Prins [15, §4]. They provide a method for computing the generating function

$$\overline{H}(x, t_1, t_2, \dots) = \sum \overline{h} x^m t_1^{m_1} t_2^{m_2} \dots,$$

where  $\bar{h}$  is the number of trees having  $n$  vertices altogether, with  $n_i$  vertices of degree  $i$ . To get the number of *homeomorphically irreducible* trees  $h$  partitioned by degree, we remove the possibility of any degree being two (letting  $t_2 = 0$ ). This involves only standard enumerative procedures and the details are omitted. We give below the equations that determine the required generating function for homeomorphically irreducible trees.<sup>9</sup>

$$\begin{aligned} P &= x(t_1 + t_3 h_2[P] + t_4 h_3[P] + \dots) \\ R &= x(t_1 P + t_3 h_3[P] + t_4 h_4[P] + \dots) \\ H &= R - a_2[P] \end{aligned}$$

**Theorem 4.2.2.** *The number of different trees in  $K_n$  of codim  $k$  is given by the above generating function*

$$H = H(x, t_1, t_3, \dots) = \sum h x^m t_1^{m_1} t_3^{m_3} \dots,$$

where  $m = n + k + 1$ ,  $m_1 = n$ , and  $\sum_{i \geq 3} m_i = k + 1$ .

We note in passing that all homeomorphically irreducible trees up to 16 vertices are depicted in [28] together with their degree partitions.

**4.3.** Roughly speaking, faces of the associahedron correspond to polygons and faces of the moduli space to labeled polygons. Both types (polytope structures) and classes (intersections of polytopes) are natural objects in the associahedron and the moduli space. We extend our idea of trees by labeling their external vertices. Unfortunately, *labeled trees* are of little use to  $\overline{\mathcal{M}}_0^n(\mathbb{R})$ ; the trees shown in Figure 14 are identical considered as labeled trees and yet distinct as faces in  $\overline{\mathcal{M}}_0^n(\mathbb{R})$ .



FIGURE 14. Identical labeled trees

However, labeled trees are *exactly* what are needed to understand the points of the *complex* moduli space  $\overline{\mathcal{M}}_0^n(\mathbb{C})$ . A rough sketch for this is as follows: The real moduli space  $\overline{\mathcal{M}}_0^n(\mathbb{R})$  comes from a configuration of labeled points on  $\mathbb{R}\mathbb{P}^1$  (viewed as a circle). Keeping track of the cyclic ordering of these points is crucial, since two adjacent labeled points can switch places only by first colliding with each other. Points on a circle give rise to the planarity of trees, and the collision/permutation of adjacent points are kept track of with the twist operation. The situation is different

<sup>9</sup>The symmetric function notation for cycle-indexes has been used (see [24]). For example, we write  $h_n[P]$  in place of  $Z(\mathbb{S}_n, P(x, t_1, t_2, \dots))$ .

for the complex case.  $\overline{\mathcal{M}}_0^n(\mathbb{C})$  is based on a configuration of labeled points on  $\mathbb{C}\mathbb{P}^1$  (viewed as a sphere). There are diffeomorphisms of the sphere which can permute any two labeled points without their need to collide, giving rise to non-planar trees. This is the fundamental reason that the underlying structures are classes for  $\overline{\mathcal{M}}_0^n(\mathbb{R})$  and trees for  $\overline{\mathcal{M}}_0^n(\mathbb{C})$ .

*Remark.* We point out a few observations about moduli spaces and trees.

1. The codim  $k$  faces of  $\overline{\mathcal{M}}_0^n(\mathbb{C})$  correspond to labeled trees with  $n$  external vertices and  $k + 1$  internal vertices. In particular, both  $\overline{\mathcal{M}}_0^n(\mathbb{R})$  and  $\overline{\mathcal{M}}_0^n(\mathbb{C})$  have the same number of zero dim cells, enumerated by binary trees with labeled external vertices. In other words, the twist operation on planar binary trees removes the restriction of planarity.

2. There are operad structures related to the moduli spaces  $\overline{\mathcal{M}}_0^n(\mathbb{R})$  [8] and  $\overline{\mathcal{M}}_0^n(\mathbb{C})$  [11], classically described in terms of labeled trees [4, §1.4]. The associahedron is related to  $A_\infty$  structures, whereas  $\overline{\mathcal{M}}_0^n(\mathbb{R})$  seems to play a similar role in Fukaya's Lagrangian Floer cohomology.

3. Kapranov [16] has defined a natural double cover of the moduli space  $\overline{\mathcal{M}}_0^n(\mathbb{R})$  by fixing one of the  $n$  distinct labeled points in  $\mathbb{R}\mathbb{P}^1$  to be  $\infty$ . Similar to  $\overline{\mathcal{M}}_0^n(\mathbb{R})$ , this double cover also has an underlying structure of labeled trees [8, §4.3] with two exceptions. First, the trees are no longer free but rooted at the label  $\infty$ . Second, twisting is allowed except along the edge containing the root.

4. The reason for these moduli spaces to be characterized by trees without degree two vertices is due to the stability condition coming from Geometric Invariant Theory [18, §8]. GIT gives a natural compactification of the space of genus zero algebraic curves which are *stable* in the sense of having only finitely many automorphisms; that is, the curves cannot have just two distinguished points.  $\square$

## 5. THE ISOTROPY GROUP

**5.1.** There is a natural action of the symmetric group  $\mathbb{S}_n$  on  $\overline{\mathcal{M}}_0^n(\mathbb{R})$  which permutes the labelings of the  $n$ -gon. This action is certainly not free; therefore, for a given face  $f$  in  $\overline{\mathcal{M}}_0^n(\mathbb{R})$ , its isotropy group  $\mathfrak{S}_f \subset \mathbb{S}_n$  need not be trivial, where

$$\mathfrak{S}_f = \{\sigma \in \mathbb{S}_n \mid \sigma(f) = f\}.$$

Given two distinct faces of  $\overline{\mathcal{M}}_0^n(\mathbb{R})$  which are of the same class, their isotropy groups are *isomorphic*; in fact, they are conjugate subgroups in  $\mathbb{S}_n$ . We wish to determine, up to isomorphism, the isotropy group of a given class; we interchangeably write  $\mathfrak{S}_f$  to denote the isotropy group of  $f$  and its isomorphism class.

**Example 5.1.1.** Let  $f$  be the face of  $\overline{\mathcal{M}}_0^8(\mathbb{R})$  given in Figure 15a; its class is 8.2.7. Its isotropy group is generated by the reflections  $\{(68), (35), (12)(83)(74)(65)\}$ .

Since the reflections commute,  $\mathfrak{S}_f$  is isomorphic to the direct product  $\mathbb{Z}_2^3$ . As discussed above, all isotropy groups of class 8.2.7 will be isomorphic. In particular, a face  $g$  of the same class, as shown in Figure 15b, will have a conjugate subgroup  $\mathfrak{S}_g = (24)(567) \cdot \mathfrak{S}_f \cdot (765)(42)$ .



FIGURE 15. Faces with conjugate subgroups

**Corollary 5.1.2.** *For a given class  $n.k.i$ , let  $\kappa$  be the number of faces in  $K_{n-1}$  of this class. The number of faces in  $\overline{\mathcal{M}}_0^n(\mathbb{R})$  of the class  $n.k.i$  is*

$$\kappa \cdot \frac{(n-1)!}{2^{k+1}}.$$

*Proof.* This immediately follows from Propositions 2.2.2 and 4.1.2.  $\square$

This can be obtained using another approach: Choose a dissected polygon representing the class  $n.k.i$ . Under all possible labelings, there are  $n!$  such polygons, many of which are identified in  $\overline{\mathcal{M}}_0^n(\mathbb{R})$ . Since the isotropy group maps the polygon to itself in the moduli space, we quotient  $n!$  by the order of the isotropy group  $|\mathfrak{S}_f|$ , where  $f$  is any face in  $\overline{\mathcal{M}}_0^n(\mathbb{R})$  of the given class. This provides another answer to for the Corollary above; combining the results, we find a solution to  $P3$  alternate to the one given in Proposition 4.1.2.

**Proposition 5.1.3.** *The number of faces in  $K_{n-1}$  of the class  $n.k.i$  is*

$$\frac{n \cdot 2^{k+1}}{|\mathfrak{S}_f|}.$$

**5.2.** The following sketches one possible algorithm for finding the group  $\mathfrak{S}_f$ . This is done *locally* (looking at each cell of the cluster under twisting) and *globally* (looking at the entire dissected polygon under the dihedral group).

**Definition 5.2.1.** For a connected graph  $G$ , the *distance* between two vertices  $x, y$  is the minimum of the lengths of paths containing  $x$  and  $y$ . The *eccentricity* of a vertex is the maximum of its distances to all other vertices. The *center* of  $G$  is the subgraph induced by the vertices of minimum eccentricity.

It is a classic result of graph theory that the center of a tree is either one vertex or one edge. Taking the dual, the center of the dissected polygon is either a cell or a diagonal.

*Non-central cells:* For each non-central cell of the polygon, observe if there exists an automorphism of the cell obtained by twisting along diagonals. If such a map exists, then this contributes  $\mathbb{Z}_2$  to  $\mathfrak{S}_f$ . Figure 16b shows the class 9.4.10 as a cluster, with the central cell shaded. Out of the four non-central cells, three of them have a  $\mathbb{Z}_2$  action (Figure 16c), contributing  $\mathbb{Z}_2^3$  to the isotropy group.

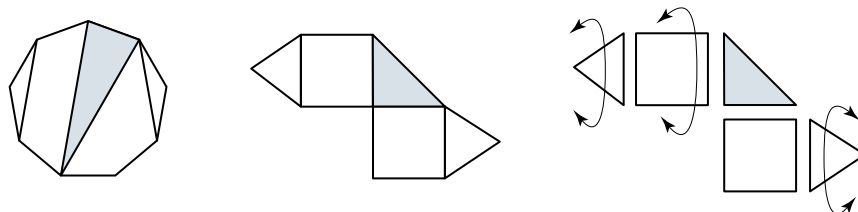


FIGURE 16. Local cells

*Central diagonal:* If the center is a diagonal, there are two possibilities: Observe whether or not there exists a (global) reflection along the central diagonal. Figure 17 shows class 8.3.8 with reflection and class 8.3.10 without.



FIGURE 17. Central diagonal

*Central cell:* If the center is a cell, there are three possibilities. Figure 18a shows class 9.5.3 with the central cell (shaded) having no symmetry. The cell could also have just a reflection action (class 9.3.11), as in Figure 18b. Finally, for an  $n$ -gon, there could be a dihedral action  $D_k$  on the central cell, where  $k$  divides  $n$ . Figure 18c shows class 9.6.4 with the  $D_3$  group action.<sup>10</sup>

Since there are no intersecting diagonals, the different twists and reflections, along with any dihedral group action, all commute. Therefore, to find the isotropy group, we look at the contribution of each local and global action and simply take their direct product. For example, the isotropy groups (up to isomorphism) for the

<sup>10</sup>Although the picture shown has obvious  $\mathbb{Z}_3$  rotation symmetry, reflection is also possible due to twisting.

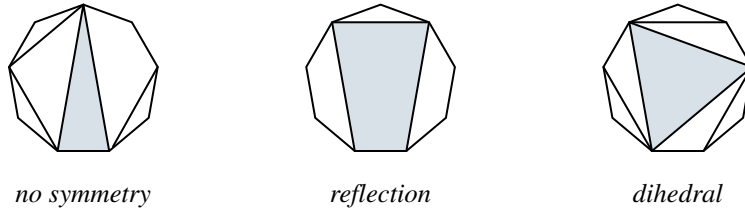


FIGURE 18. Central cell

polygons of Figure 18 are  $\mathbb{Z}_2^4$ ,  $\mathbb{Z}_2^4$ , and  $\mathbb{Z}_2^3 \times D_3$ , respectively. Using Proposition 5.1.3, we calculate  $\kappa$  for each of the classes to be 36, 9, and 24, respectively, matching the values obtained from Proposition 4.1.2.

*Remark.* Each class corresponds to a polytope. By definition, each element of the isotropy group maps the polytope to itself; but what type of map is it? Using Figure 15a as an example of a face  $f$ , we show how the generators of  $\mathfrak{S}_f$  act on the polytope. Note that the polytope structure of  $f$  is a cube, the product of three line segments, as labeled in Figure 19. The actions of the three generators of  $\mathfrak{S}_f$  given in Example 5.1.1 are the reflections along the shaded planes.

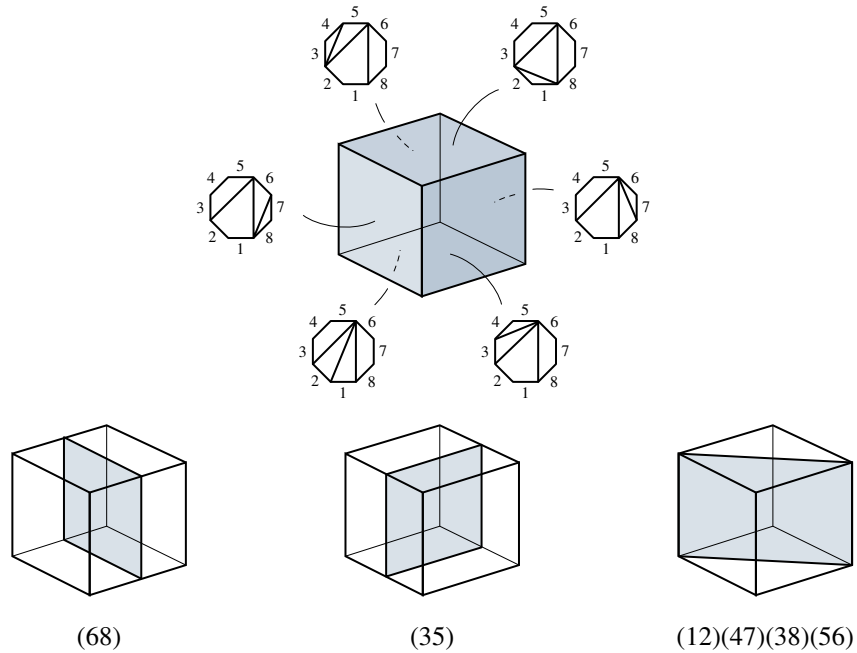


FIGURE 19. Labeled polytope

6. APPLICATIONS

**6.1.** We first point out a few interesting similarities to classical combinatorics [7, §1.15]. As noted above, partitioning of an  $n$ -gon using  $k$  diagonals corresponds to using  $k$  sets of brackets meaningfully on  $n - 1$  *non-commutative* variables (see Figure 20).

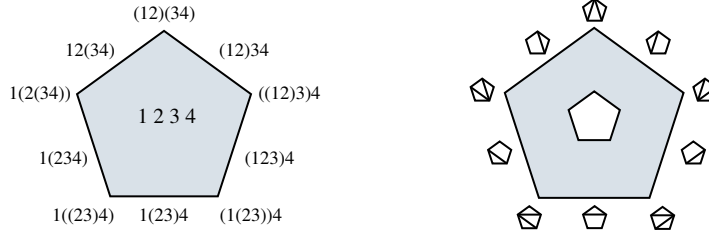


FIGURE 20. Parentheses and Polygons

The *Generalized bracketing problem of Schröder* is to find the number  $s_n$  of different bracketings of  $n$  variables using an arbitrary number of brackets (where each bracket must contain at least two elements). Lemma 2.2.1 gives us the number of different bracketing for a fixed set of  $k$  brackets. Summing up, we find

$$s_n = \sum_{k=0}^{n-2} \frac{1}{k+1} \binom{n+k}{k} \binom{n-2}{k}.$$

The *Wedderburn-Etherington commutative bracketing problem* is to find the number  $w_n$  of ways of using  $n - 2$  sets of brackets meaningfully on  $n$  *commutative* variables. In other words, it is the number of different *bracketings* that arise from commuting binary subproducts. It is not too hard to see that  $w_n$  gives the number of  $(n + 1)$ -gons with maximal diagonals rooted at an outside edge, identified up to reflection along the root edge and twisting along diagonals, but *not* rotation. It follows that  $w_n = a_{n-1,n}$  (see Table 2). Figure 21 shows  $w_4 = 2$  and  $w_5 = 3$  as polygon and bracketing representations.

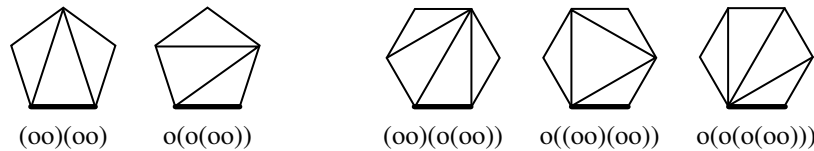


FIGURE 21. Representations of  $w_4$  and  $w_5$

*Remark.* The coefficients of the generating function of Equation 3.1 generalize the Wedderburn-Etherington numbers: The possible ways of using  $k$  brackets on  $n$  commutative variables is  $a_{k+1,n}$ .

**6.2.** We mention two occurrences outside mathematics that encode information using labeled trees. The first is in biology; in particular, the areas of genetics and evolution [20]. The theory of evolution conjectures that there exist links between certain species to common ancestors using the evidence from protein sequences. An evolutionary tree, or *phylogeny*, is a means of organizing this data: The external (labeled) vertices represent species for which data is available whereas the internal (unlabeled) vertices are the hypothetical ancestors for which no direct evidence is known. Phylogenies usually have no vertices of degree two. The following enumerates the number of phylogenies having a fixed set of leaves.

**Proposition 6.2.1.** [10, §2] *For  $n$  external vertices, the number  $T_n$  of labeled trees is given by the following recurrence relation, where  $T_2 = T_1 = 1$ :*

$$T_n = (2 - n)T_{n-1} + \sum_{1 \leq i \leq n-2} T_{i+1}T_{n-i} \binom{n-1}{i}.$$

*Remark.* A few observations follow:

1. Just as the generalized bracketing problem of Schröder sums over all cells of  $K_n$ , the proposition above sums over all the cells of  $\overline{\mathcal{M}}_0^n(\mathbb{C})$ .
2. A *rooted* phylogeny is a rooted labeled tree where the root does not receive a label. The root of a phylogeny represents the ancestor of all organisms of the tree. For  $n$  labeled external vertices, the number  $P_n$  of distinct rooted phylogenies is  $P_n = T_{n+1}$  [10, §2].
3. There exist many possible metrics on phylogenetic trees [9]. It was also noted in [20] that one can give lengths to the edges of labeled trees, making them *weighted*, which hold data on the time estimate of evolution taking place between two species of the tree. Recently, a space of phylogenetic trees was constructed, closely related to the ‘dual’ of  $\overline{\mathcal{M}}_0^n(\mathbb{R})$  [3]; the metric on this tree space inherits some properties from the natural metric on  $\overline{\mathcal{M}}_0^n(\mathbb{R})$  [8, §2.2].
4. The idea of phylogeny even extends to literature, in understanding the authenticity of the manuscripts of *The Canterbury Tales* [1]. □

**6.3.** Another appearance of labeled trees is in physics; in particular, the quantum theory of angular momentum. Given a system of  $n$  independent parts, each with its own angular momentum, the theory deals with constructing the total angular momentum by coupling the given  $n$  momenta sequentially in pairs using  $SU(2)$  Wigner coefficients. Biedenharn and Louck further relate this to the Racah-Wigner algebra and the 6- $j$  symbols [2, §5]. Enumerating the various *binary coupling schemes* gives a total of  $c_n$  possibilities, thought of as counting maximal bracketings on  $n$  variables (zero dim cells of  $K_n$ ). Permuting two angular momenta implies a phase change in their *state vectors*. Considering binary coupling schemes over all such permutations yield  $n! \cdot c_n$  possibilities (zero dim cells in  $n!$  copies of  $K_n$ ). However, in quantum

physics it is not possible to distinguish state vectors differing by phase factors; schemes are identified by commuting binary subproducts. This yields  $(2n - 3)!!$  possible coupling schemes (zero dim cells in  $\overline{\mathcal{M}}_0^{n+1}(\mathbb{R})$ ). As noted, the idea of binary coupling closely follows the gluing of associahedra to form the moduli space, at least in the zero dimensional case. Although combinatorially the idea of coupling momenta can be generalized beyond binary pairs (by possibly counting the codim  $k$  cells of moduli spaces), the meaning of this in the context of theoretical physics is not yet well understood.

*Acknowledgments.* The authors would like to acknowledge their indebtedness to, and admiration for, the work of Professor Arthur Cayley, who not only addressed a dissection problem similar to the one in this paper, but also laid the foundations for the enumerative study of tree-like structures in general. This pioneering work is all the more remarkable in that it was only a small part of the mathematical output of this eminent Victorian.

3	4	5	6	7	8	9	10	Total
3								5
1	1							5
		1						1
4								14
2	1							21
1		1						6
	2							3
			1					1
5								42
3	1							84
2		1						28
1	2							28
	1	2						7
1			1					7
				1				1
6								132
4	1							330
3		1						120
2		2						180
2			1					36
1	1	1						72
	3							12
1				1				8
	1		1					8
		2						4
					1			1
7								429
5	1							1287
3	2							990
3			1					165
2	1	1						495
3		1						495
1	3							165
2				1				45
	2	1						45
1					1			9
	1			1				9
		1	1					9
						1		1
8								1430
6	1							5005
5		1						2002
4	2							5005
4			1					715
3	1	1						2860
2	3							1430
3				1				220
2		2						330
2	1		1					660
1	2	1						660
	4							55
2					1			55
1	1			1				110
1		1	1					110
	2		1					55
	1	2						55
1						1		10
	1				1			10
		1		1				10
			2					5
							1	1

TABLE 1. Dissections of the  $n$ -gon ( $n = 5, \dots, 10$ )

	1	2	3	4	5	6	7	8	9	10	11	12
2	1											
3	1	1										
4	1	3	2									
5	1	5	8	3								
6	1	8	22	20	6							
7	1	11	46	73	49	11						
8	1	15	87	206	233	119	23					
9	1	19	147	485	807	689	288	46				
10	1	24	236	1021	2320	2891	1988	696	98			
11	1	29	356	1960	5795	9800	9737	5561	1681	207		
12	1	35	520	3525	13088	28586	38216	31350	15322	4062	451	
13	1	41	730	5989	27224	74280	127465	139901	97552	41558	9821	983

TABLE 2.  $a_{m,n}$ 

	1	2	3	4	5	6	7	8	9	10	11
2	1										
3	1	2									
4	1	5	5								
5	1	9	21	14							
6	1	14	56	84	42						
7	1	20	120	300	330	132					
8	1	27	225	825	1485	1287	429				
9	1	35	385	1925	5005	7007	5005	1430			
10	1	44	616	4004	14014	28028	32032	19448	4862		
11	1	54	936	7644	34398	91728	148512	143208	75582	16796	
12	1	65	1365	13650	76440	259896	556920	755820	629850	293930	58786

TABLE 3.  $v_{m,n}$ 

	1	2	3	4	5	6	7	8	9	10	11	12
3	1											
4	1	1										
5	1	2	2									
6	1	3	7	4								
7	1	4	15	18	7							
8	1	5	28	57	49	14						
9	1	6	45	138	196	123	29					
10	1	7	69	288	601	626	313	60				
11	1	8	98	540	1533	2322	1899	778	127			
12	1	9	136	943	3468	7095	8362	5565	1936	275		
13	1	10	180	1544	7124	18813	29741	28350	15880	4776	598	
14	1	11	235	2419	13635	44868	90869	115642	92210	44433	11777	1320

TABLE 4.  $b_{m,n}$ 

	1	2	3	4	5	6	7	8	9	10	11	12	13
3	1												
4	1	1											
5	1	1	1										
6	1	2	3	2									
7	1	2	6	5	2								
8	1	3	11	17	12	4							
9	1	3	17	37	44	23	6						
10	1	4	26	78	131	118	52	11					
11	1	4	36	140	325	410	298	109	18				
12	1	5	50	248	728	1249	1279	766	244	37			
13	1	5	65	396	1476	3246	4462	3763	1921	532	66		
14	1	6	85	624	2811	7717	13497	15198	10920	4843	1196	135	
15	1	6	106	929	5032	16773	36384	52041	49577	30848	12068	2671	265

TABLE 5.  $f_{m,n}$

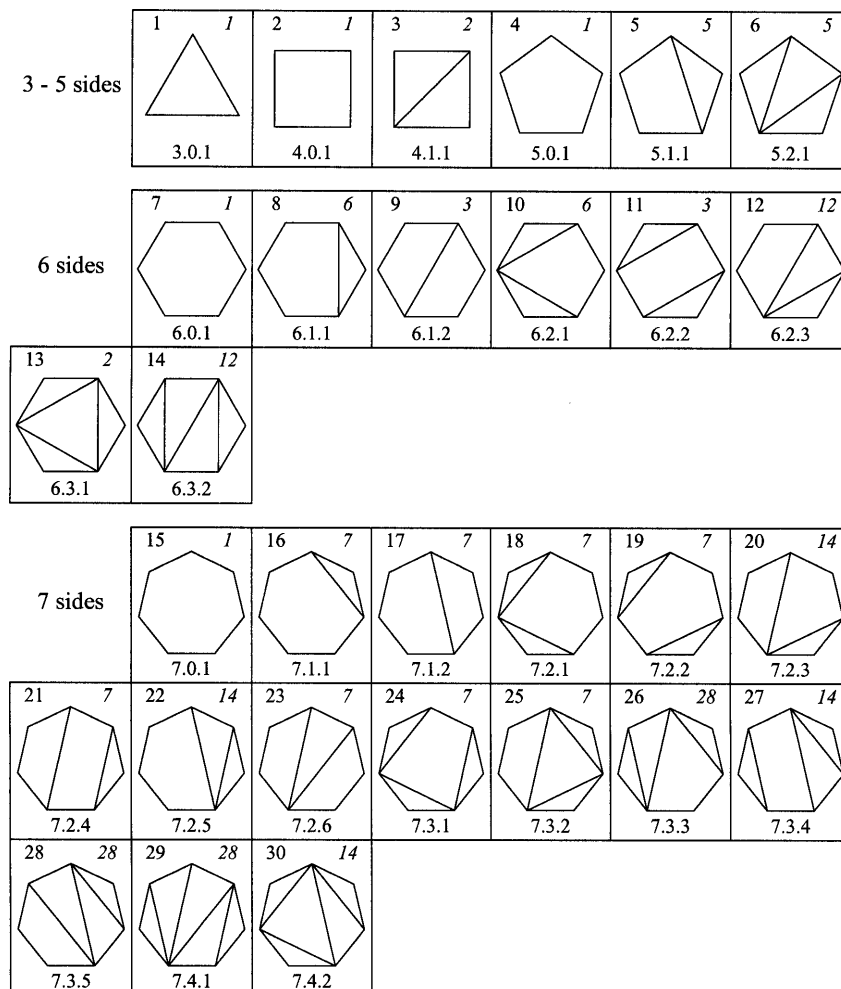


FIGURE 22. Dissected 3-gons through 7-gons

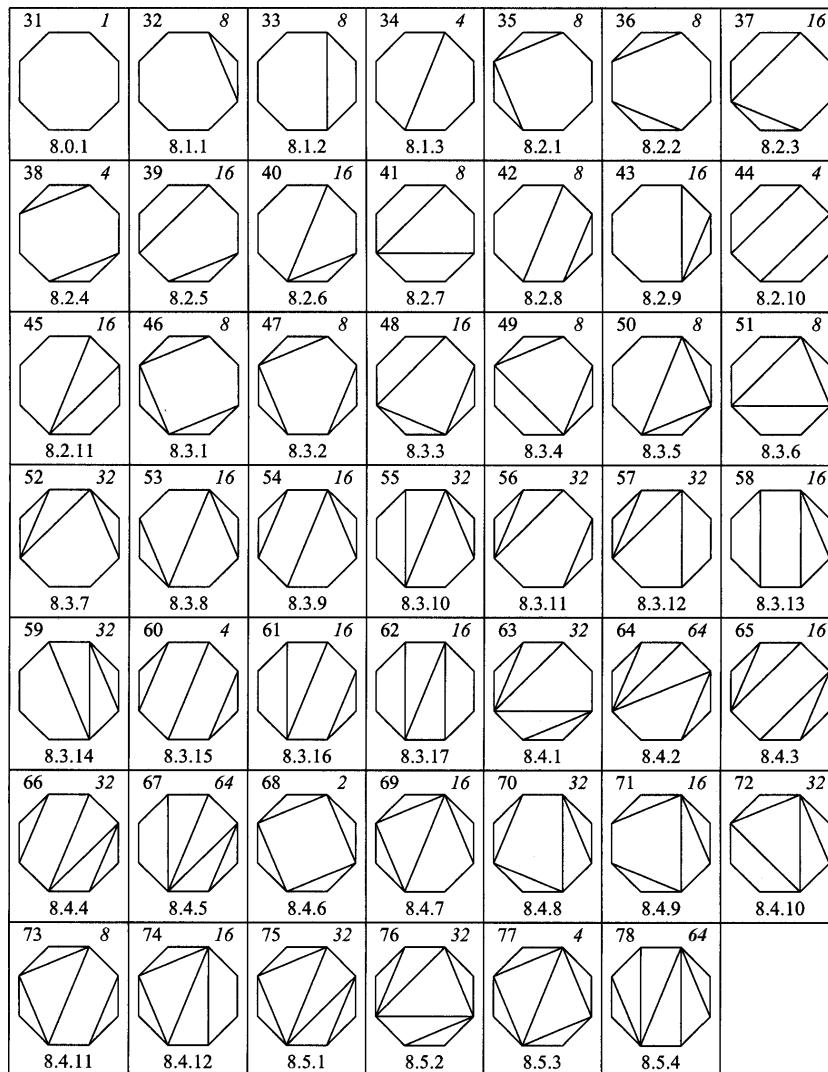


FIGURE 23. Dissected 8-gons

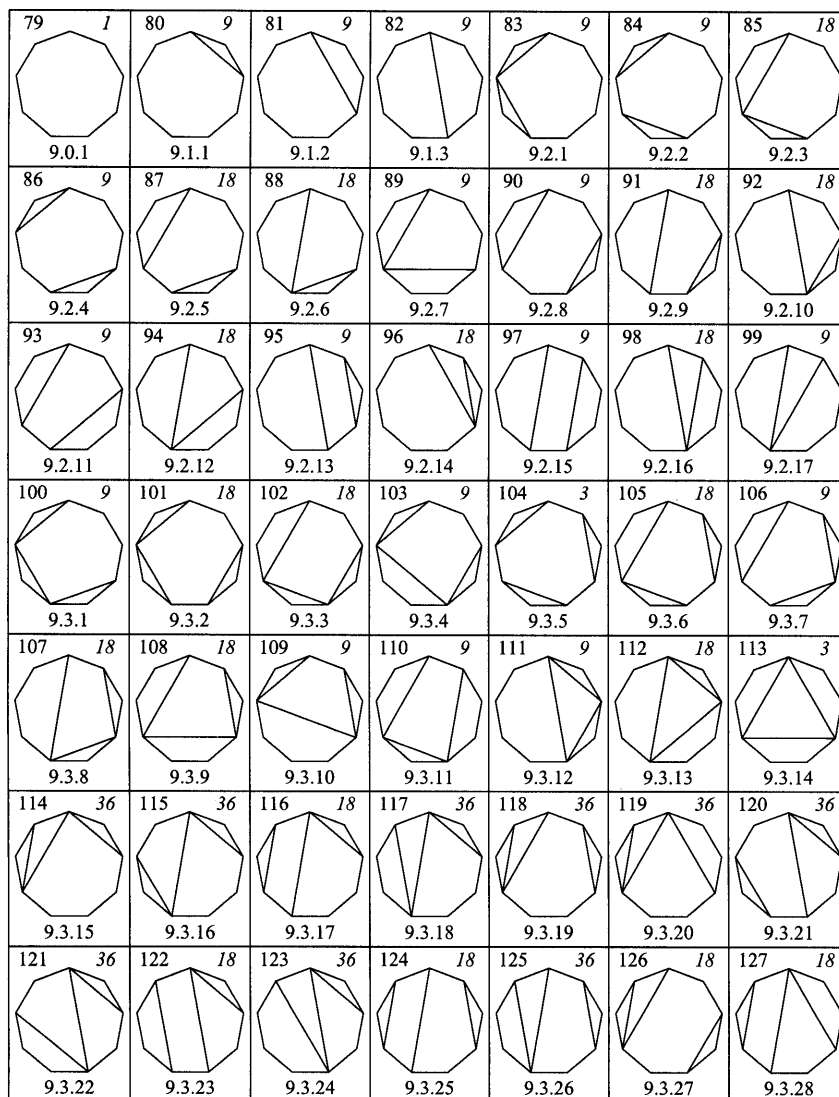


FIGURE 24. Dissected 9-gons, part I

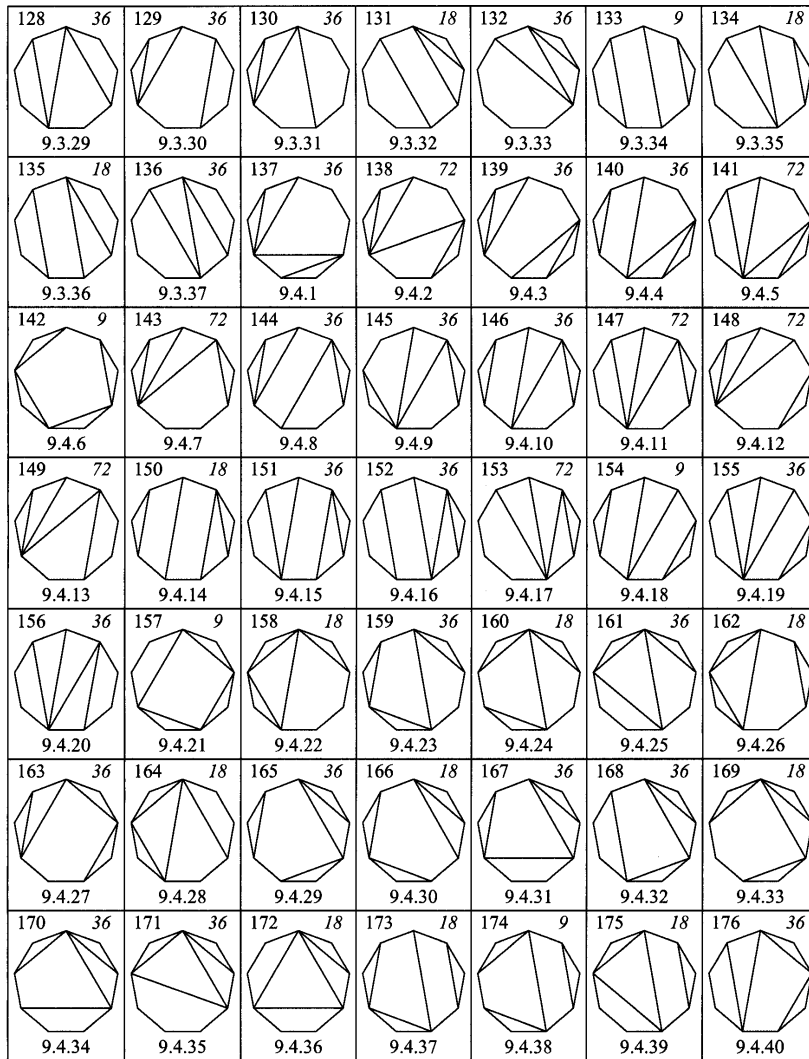


FIGURE 25. Dissected 9-gons, part II

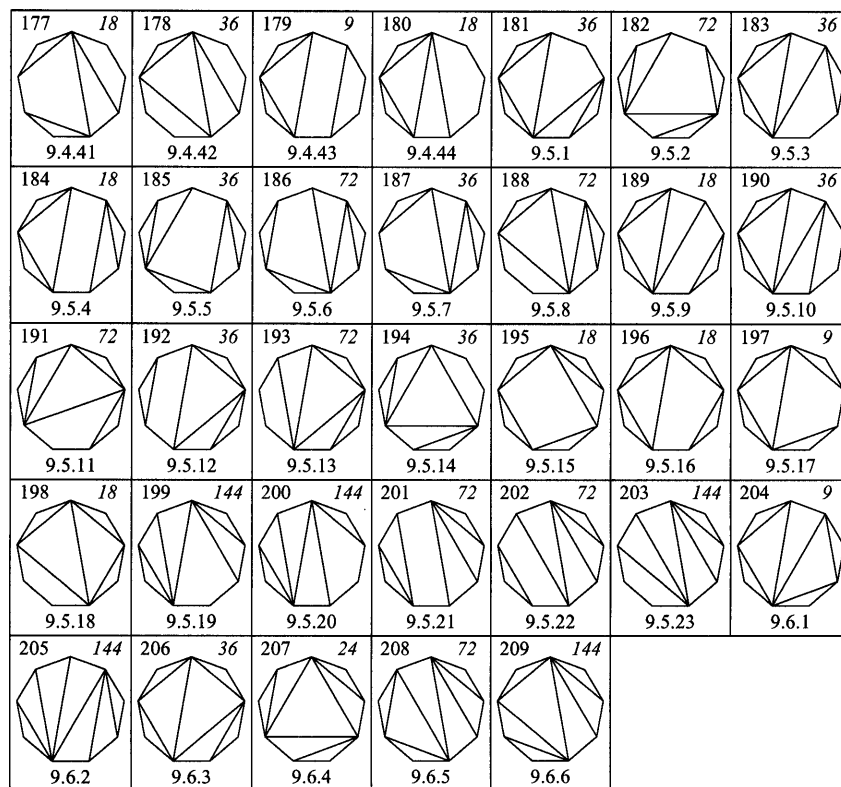


FIGURE 26. Dissected 9-gons, part III

## REFERENCES

1. A. Barbrook, N. Blake, *et al.*, *The phylogeny of The Canterbury Tales*, Nature **394** (1998) 839.
2. L. C. Biedenharn, J. D. Louck, **The Racah-Wigner Algebra in Quantum Theory**, Encyclopedia of mathematics and its applications, Addison-Wesley Publishing (1981).
3. L. J. Billera, S. P. Holmes, K. Vogtmann, *Geometry of the Space of Phylogenetic Trees*, (2000) preprint.
4. J. M. Boardman, R. M. Vogt, **Homotopy invariant algebraic structures on topological spaces**, Lecture Notes in Math. **347** (1973).
5. H. R. Brahana, A. M. Coble, *Maps of twelve countries with five sides with a group of order 120 containing an Ikosahedral subgroup*, Amer. J. Math. **48** (1926) 1-20.
6. A. Cayley, *On the partitions of a polygon*, Proc. Lond. Math. Soc. **22** (1890-91) 237-262.
7. L. Comtet, **Advanced Combinatorics**, D. Reidel Publishing (1974).
8. S. L. Devadoss, *Tessellations of moduli spaces and the mosaic operad*, Contemp. Math. **239** (1999) 91-114.
9. L. R. Foulds, R. W. Robinson, *Comparison of phylogenetic trees*, Math. Biosci. **53** (1981) 131-147.
10. L. R. Foulds, R. W. Robinson, *Enumeration of phylogenetic trees without points of degree two*, Ars Combin. **17A** (1984) 169-183.
11. V. A. Ginzburg, M. M. Kapranov, *Kozul duality for operads*, Duke Math. J. **76** (1994) 203-272.
12. A. Grothendieck, *Esquisse d'un programme*, **Geometric Galois actions, I**, Lond. Math. Soc. Lecture Notes **242**, (1997) 5-48.
13. I. P. Goulden, D. M. Jackson, **Combinatorial Enumeration**, John Wiley and Sons (1983).
14. F. Harary, E. M. Palmer, **Graphical Enumeration**, Academic Press (1973).
15. F. Harary, G. Prins, *The number of homeomorphically irreducible trees, and other species*, Acta Math. **101** (1959) 141-162.
16. M. M. Kapranov, *The permutoassociahedron, MacLane's coherence theorem, and asymptotic zones for the KZ equation*, J. Pure Appl. Alg. **85** (1993) 119-142.
17. C. Lee, *The associahedron and triangulations of the n-gon*, European J. Combin. **10** (1989) 551-560.
18. D. Mumford, J. Fogarty, F. Kirwan, **Geometric Invariant Theory** 3<sup>ed</sup>, Springer-Verlag (1994).
19. R. Otter, *The number of trees*, Acta Math. **49** (1948) 583 - 599.
20. R. D. M. Page, E. C. Holmes, **Molecular Evolution: A Phylogenetic Approach**, Blackwell Science (1998).
21. G. Pólya, *Kombinatorische Anzahlbestimmungen für Gruppen Graphen und chemische Verbindungen*, Acta Math. **68** (1937) 142-245.
22. G. Pólya, R. C. Read, **Combinatorial Enumeration of Groups, Graphs, and Chemical Compounds**, Springer-Verlag (1987).
23. J. H. Przytycki, A. S. Sikora, *Polygon dissections and Euler, Fuss, Kirkman, and Cayley numbers*, (1997) preprint co/9811086.
24. R. C. Read, *The use of S-functions in combinatorial analysis*, Canad. J. Math. **20** (1968) 808 - 841.
25. R. C. Read, *On general dissections of a polygon*, Aeq. Math. **18** (1978) 370 - 388.
26. R. C. Read, *A survey of graph generation techniques*, Lecture Notes in Math. **884** (1981) 77-89.

27. R. C. Read, *Enumeration, Graph Connections*: Chapter 2, Oxford Science Pub. (1997).
28. R. C. Read, R. J. Wilson, **An Atlas of Graphs**, Oxford University Press (1999).
29. R. P. Stanley, **Enumerative Combinatorics, Volume 2** Cambridge University Press (1999).
30. J. D. Stasheff, *Homotopy associativity of  $H$ -spaces I*, Trans. Amer. Math. Soc. **108** (1963) 275-292.

DEPARTMENT OF MATHEMATICS, OHIO STATE UNIVERSITY, COLUMBUS, OHIO  
*E-mail address*: `devadoss@math.ohio-state.edu`

DEPARTMENT OF COMBINATORICS AND OPTIMIZATION, UNIVERSITY OF WATERLOO, CANADA  
*E-mail address*: `rcread@math.uwaterloo.ca`